

# Electron Gas-Impurity Ion Mutual Interactions in N-Type Mixed Semiconductors

Sung-rak Hong · Robert J. Sirko

N형 혼합반도체에서 Electron Gas와  
Impurity Ion 과의 상호작용

홍 성 략 · Robert J. Sirko

## Summary

We have studied theoretically the formalism describing the nature of coupling in a polar semiconductor binary alloy-electron gas system, and have carried out numerical calculations for a representative real crystal in the long wavelength limit.

## (1) INTRODUCTION

It is well known that in doped polar semiconductors the LO phonon can couple to the electron plasma when the electron plasma frequency is comparable to the LO phonon frequency (Singwi, 1966; Mooradian, 1966; Mooradian, 1969).

This is necessarily a coupling that exists only in the long wavelength limit where the electrons can exhibit their collective oscillations. The characteristic parameter defining the region of coupling is the Debye inverse screening length,  $K_D$ , at finite temperatures. Generally the electron plasma exists for wave vectors  $K$  such that  $K < K_D$ , while for shorter wavelengths the plasma breaks up into single particle excitations. Since  $K$  is typically only a very small fraction of any reciprocal lattice vector, any theory accounting for the LO phonon-plasma coupling may safely neglect dispersion of the phonons, although the plasma induced dispersion may play an important

role in the resulting mixed modes (Katayama, 1975).

In the above description only a single phonon mode—the  $k=0$  LO phonon—is significant in considering lattice-electron gas interactions. Crystals such as n-GaAs and n-GaP are representative types. (Here we note that the dopant impurities may be safely ignored in all further considerations since their concentration is low—typically on the order of  $10^{18}$  cm<sup>-3</sup> or less—and their mass may be large so that the optical phonon spectrum of the lattice shows no effect of their presence.) However, the picture is somewhat more involved when one considers a binary alloy such as GaAs<sub>1-x</sub>P<sub>x</sub>, where either of two isoelectronic ions occupy every available equivalent lattice site. In the low concentration limit,  $x \ll 1$ , there exist well defined localized vibration modes associated with the widely separated light ions if the isotopic mass difference of the two ion types is significant (Montroll, 1955), and the characteristic local mode

frequency is then substantially higher than the  $k=0$  LO phonon frequency associated with the host lattice. For example, in  $\text{GaAs}_{1-x}\text{P}_x$  with  $x \ll 1$ , the LO phonon frequency of the host GaAs lattice is approximately  $294 \text{ cm}^{-1}$  while the local mode frequency associated with the individual P ions is approximately  $350 \text{ cm}^{-1}$ . These local modes, while, as one would expect, only very weakly mutually coupled by their dipole-dipole interactions in the low concentration limit, may interact significantly through the electron gas in a manner analogous to the LO phonon-plasma coupling described above (Sirko, 1975; Sham, 1967).

Thus we are led to view the LO phonon-plasma and the local mode-plasma interacting systems as special limiting cases of a doped binary alloy polar semiconductor; in the former case,  $x$ , the impurity ion concentration, is exactly zero, while in the latter case  $x \ll 1$ , and, indeed, the host lattice is conveniently ignored. We now proceed to treat the binary alloy-electron gas system over the entire range  $0 \leq x \leq 1$ .

The outline of the paper is as follows. In section II we develop Green's functions appropriate to the system of interest by first treating special subsystems, and generalizing to the alloy-electron system. We obtain general wave vector dependent formal results for the Green's functions of interest, from which the resonant modes of the interacting system are directly derived. We specialize these results to obtain the infinite wavelength limits, for which both the Green's functions and the resonant frequencies have simple algebraic structure. In section III we derive an expression for the dielectric constant of the system utilizing the formalism of section II, and in section IV we discuss extensions of the present work that are now being investigated by the authors.

## II. Formalism and Coupled Modes

We consider a lattice with either of two ion types A or B at each equivalent lattice site. Associated with each A and B ion is a third ion of opposite charge—there are thus two ions per primitive cell, giving rise to the optical phonon spectrum. The presence of this third ion type is nowhere explicitly acknowledged, but when dealing with A or B ion displacement, of course it is the relative displacement from the center of mass of the ion pair in a primitive cell to which we are referring. Similarly we refer to the effective mass of the A ion and its oppositely charged partner simply as  $m_A$ , while  $m_B$  has an equivalent definition. We suppose the two ion types, A and B, to be electronically identical, and with no loss in generality we take  $m_A$  to be less than  $m_B$ .

We suppose there is a concentration,  $n_e$ , of doping electrons in a parabolic conduction band characterized by an effective mass  $m^*$ . The electron gas gives rise to plasma oscillations with the long wavelength plasma frequency given by

$$\omega_p^2 = 4\pi n_e e^2 / \epsilon_\infty m^* \dots \dots \dots (1)$$

Here  $\epsilon_\infty$  is the high frequency dielectric constant and  $e$  is the electron charge. We write the Hamiltonian of such a system as

$$H = H_0 + H_I, \dots \dots \dots (2)$$

where  $H_0$  represents the three zero order elementary excitations of the system,

$$H_0 = H_A + H_B + H, \dots \dots \dots (3)$$

and  $H_I$  contains all the mutual interaction terms. We have

$$H_A = \omega_A \sum_{\vec{l}} C_A(\vec{l}) a_{\vec{l}}^{\dagger} a_{\vec{l}}, \dots \dots \dots (4)$$

with  $\omega_A$  the vibration frequency of an A ion embedded in an empty lattice (except for its oppositely charged partner), and  $a_{\vec{l}}^{\dagger} (a_{\vec{l}})$  is the destruction (creation) operator of a localized mode at the  $\vec{l}$  lattice site with displacement along

the  $\mu$  Cartesian component. The occupation number  $C_A(I)$  is defined by

$$C_A(I) = \begin{cases} 1, & \text{if an A ion is at site A} \\ 0, & \text{otherwise} \end{cases} \quad \dots\dots(5)$$

Of course  $\omega_A$  is just the local mode frequency in the low A ion concentration limit. We have set  $\hbar=1$  and will use this convention throughout. Similarly,

$$H_B = \omega_B \sum_{I\mu} C_B(I) b_{I\mu}^\dagger b_{I\mu}, \quad \dots\dots(6)$$

where  $\omega_B$ ,  $b_{I\mu}^\dagger$ ,  $b_{I\mu}$  and  $C_B(I)$  have definitions analogous to those given above. The assumption that either an A or B type ion is present at each lattice site implies that  $C_A(I) + C_B(I) = 1$ , for all  $I$ , or equivalently

$$X_A + X_B = 1, \quad \dots\dots(7)$$

where  $X_A(X_B)$  is the concentration of the A (B) ions. The doping electrons in the conduction band give rise to the term

$$H_E = \frac{1}{2m^*} \sum_{\vec{k}} K^2 C_{\vec{k}}^\dagger C_{\vec{k}}, \quad \dots\dots(8)$$

where  $\vec{k}$  is the electron wave vector and  $C_{\vec{k}}^\dagger$  ( $C_{\vec{k}}$ ) is the electron destruction (creation) operator.

The interaction term may be written as

$$H_I = H_{AA} + H_{BB} + H_{AB} + H_{AE} + H_{BE} + H_{EE}, \quad \dots\dots(9)$$

Here  $H_{AA}$  is the A ion interionic dipole-dipole interaction,  $H_{AE}$  is the A ion-electron interaction and  $H_{EE}$  is the electron-electron Coulomb interaction. The remaining terms can be similarly described. One thus writes

$$H_{AA} = \frac{1}{2} \sum_{I'\mu'} \sum_{I\mu} C_A(I) C_A(I') \Phi_{\mu\mu'}(II') u_{\mu}^A(I) u_{\mu'}^A(I'), \quad \dots\dots(10)$$

where  $\Phi_{\mu\mu'}(II')$  is the second derivative of the interionic potential energy and  $u_{\mu}(I)$  is the  $\mu$  component of the displacement of the ion at site  $I$ . The prime in the summation over  $I'$  indicates exclusion of the  $I'=I$  term, which itself was implicitly included in the zero order term  $H_A$ ; it provides the potential well in which the

isolated ion oscillates at frequency  $\omega_A$ .

The ion displacements can be written as

$$u_{\mu}^A(I) = \frac{1}{\sqrt{2m_A\omega_A}} (a_{I\mu}^+ + a_{I\mu}^-), \quad \dots\dots(11)$$

and  $\Phi_{\mu\mu'}(II')$  is given by

$$\Phi_{\mu\mu'}(II') = -e^{*2} \frac{\partial^2}{\partial x_{\mu} \partial x_{\mu'}} \left( \frac{1}{r} \right) \Big|_{r=|x(I)-x(I')|}, \quad \dots\dots(12)$$

where  $e^*$  is the ion effective charge. Similarly, we have

$$H_{BB} = \frac{1}{2} \sum_{I'\mu'} \sum_{I\mu} C_B(I) C_B(I') \Phi_{\mu\mu'}(II') u_{\mu}^B(I) u_{\mu'}^B(I'), \quad \dots\dots(13)$$

and

$$H_{AB} = \sum_{I'\mu'} \sum_{I\mu} C_A(I) C_B(I') \Phi_{\mu\mu'}(II') u_{\mu}^A(I) u_{\mu'}^B(I'), \quad \dots\dots(14)$$

The restriction on  $I'$  is relaxed in the last term as the occupation numbers assure that the  $I'=I$  term does not contribute to the sum.

The factor of 1/2 is also not present in Eq. (14) since there is no double counting.

The electron-A ion term arises from the interaction of the dipole at ion site  $I$  with the local electric field,  $\vec{E}(I)$ , that results from electron density fluctuations throughout the crystal. With

$$H_{AB} = -e^* \sum_{I\mu} C_A(I) u_{\mu}(I) E_{\mu}(I)$$

and

$$E_{\mu}(\vec{R}) = -\frac{e}{\epsilon_{\infty}} \frac{\partial}{\partial R_{\mu}} \int d^3x \frac{\psi^+(\vec{x})\psi(\vec{x})}{|\vec{x}-\vec{R}|}, \quad \dots\dots(15)$$

we find by using Eqs. (11) and (15) that in terms of the creation and destruction operators

$$H_{AE} = i\gamma_A \sum_{I\mu} \sum_{\vec{k}\vec{q}} C_A(I) (a_{I\mu}^+ + a_{I\mu}^-) \frac{q_{\mu}}{q^2} C_{\vec{k}+\vec{q}}^\dagger C_{\vec{k}} e^{-i\vec{q}\cdot I}, \quad \dots\dots(16)$$

We have used  $\psi(\vec{x}) = \sum_{\vec{k}} C_{\vec{k}} e^{i\vec{k}\cdot\vec{x}}$  (assuming a sample of unit volume).

The coupling constant  $\gamma_A$  is given by

$$\gamma_A = (4\pi e e^* / \epsilon_{\infty}) (1/2m_A\omega_A)^{1/2}, \quad \dots\dots(17)$$

Of course,

$$H_{BE} = i\gamma_B \sum_{l\mu} \sum_{\vec{k}\vec{q}} C_B(l) (b_{l\mu}^+ + b_{l\mu})$$

$$\frac{q_\mu}{q^2} C_{\vec{k}\vec{q}}^+ C_{\vec{k}}^- e^{-i\vec{q}\cdot\vec{l}} \dots \dots \dots (18)$$

Lastly the electron-electron interaction is just

$$H_{EE} = \frac{1}{2} \iint d^3x d^3x' \psi^+(\vec{x}) \psi(\vec{x}')$$

$$V(|\vec{x}-\vec{x}'|) \psi(\vec{x}') \psi(\vec{x}),$$

where  $V(|\vec{x}-\vec{x}'|)$  is the screened Coulomb potential

$$V(|\vec{x}-\vec{x}'|) = -\frac{e^2}{\epsilon_\infty |\vec{x}-\vec{x}'|}$$

Expressing  $V(|\vec{x}|)$  in terms of its Fourier transform

$$V(x) = \frac{4\pi e^2}{\epsilon_\infty} \sum_{\vec{K}} \frac{e^{i\vec{K}\cdot\vec{x}}}{K^2} \dots \dots \dots (19)$$

and the field operators  $\psi$  and  $\psi^+$  in terms of the destruction and creation operators  $C_K$  and  $C_K^+$ , we have

$$H_{EE} = \frac{1}{2} \sum_{\vec{K}\vec{K}'\vec{q}} V_C(\vec{q}) C_{K+q}^+ C_{\vec{K}'-\vec{q}}^+ C_{\vec{K}'} C_{\vec{K}} \dots \dots \dots (20)$$

where  $V_C(q) = 4\pi e^2 / \epsilon_\infty q^2$ .

Since the full system we have just introduced is inherently complicated, we will find it convenient to begin our analysis by treating a simplified subsystem consisting of only a concentration  $X_A$  of A ions randomly located on an empty lattice with no electrons present (case (i) below). Subsequently we treat (ii) the two ion (A and B) alloy without doping electrons and, lastly, (iii) the full alloy-electron gas system. This procedure will be useful in building a complete description of the full system as well as setting forth the calculational procedures and definitions used throughout this paper.

(i) In the present case the system is described simply by  $H = H_A + H_{AA}$ . Here the triply degenerate localized vibration modes are the zero order excitations of the system, and their mutual interactions are the perturbations that will be

seen to split the modes into longitudinal and transverse components. While this system is easily treated using lattice dynamics, we proceed by calculating the A ion displacement Green's function defined by

$$D^A(l\mu\tau, l'\mu'\tau') = -\langle T_\tau [\varphi_\mu^A(l\tau) \varphi_{\mu'}^A(l'\tau')] \rangle \dots \dots \dots (21)$$

Here  $\tau$  is an imaginary time,  $T_\tau$  is the Wick's imaginary time ordering operator and  $\varphi_\mu^A(l\tau)$  is the Heisenberg operator

$$\varphi_\mu^A(l\tau) = e^{(H_A + H_{AA})\tau} \varphi_\mu^A(l) e^{-(H_A + H_{AA})\tau} \dots \dots \dots (22)$$

with

$$\varphi_\mu^A(l) = a_\mu^+ + a_{l\mu} \dots \dots \dots (23)$$

The angular brackets indicate thermal averaging. As usual  $D^A$  may be expanded in terms of powers of  $H_{AA}$  and the zero order propagator,  $D_0$ , obtained by letting  $H_{AA} \rightarrow 0$  in Eqs. (21) and (22).

The standard result for  $D_0^A$  (Abrikosov, 1965) is

$$D_0^A(l\mu, l'\mu'; i\omega_n) = -\partial_{ll'} \partial_{\mu\mu'} \left( \frac{2\omega_A}{\omega_n^2 - \omega_A^2} \right) \dots \dots \dots (24)$$

where  $D^A(l\mu, l'\mu'; i\omega_n)$  is the Fourier transform of the imaginary time propagator introduced in Eq. (21) with the defining relation

$$D^A(l\mu\tau, l'\mu'\tau') = \beta^{-1} \sum_{n \text{ even}} e^{-i\omega_n(\tau-\tau')} D^A(l\mu, l'\mu'; \omega_n) \dots \dots (25)$$

Here  $\beta = (K_B T)^{-1}$  and  $K_B$  is Boltzmann's constant.

Straight forward application of Wick's theorem to the propagator defined in Eq. (21) leads to the expansion

$$D^A(l\mu, l'\mu'; i\omega_n) = D_0^A(l\mu, l'\mu'; i\omega_n)$$

$$+ \frac{1}{2m_A \omega_A} \sum_{l_1 l_1'} C_A(l_1)$$

$$C_A(l_1') \Phi_{\mu_1 \mu_1'}(l_1 l_1')$$

$$\times D_0^A(l\mu, l_1 \mu_1; i\omega_n)$$

$$D_0^A(l_1' \mu_1' l' \mu'; i\omega_n)$$

$$\begin{aligned}
 & + \frac{1}{(2m_A\omega_A)^2} \sum_{l_1 l_1'} \sum_{l_2 l_2'} \\
 & C_A(l_1) C_A(l_1') C_A(l_2) C_A(l_2') \\
 & \times \Phi_{\mu_1 \mu_1'}(l_1 l_1') \Phi_{\mu_2 \mu_2'}(l_2 l_2') \times D_0^A(l\mu, l_1 \mu_1; i\omega_n) \\
 & D_0^A(l_1' \mu_1', l_2 \mu_2; i\omega_n) \\
 & \times D_0^A(l_2' \mu_2', l' \mu'; i\omega_n) + \dots \dots \dots (26)
 \end{aligned}$$

Further progress requires some method of dealing with the random configuration of A ions. We express our ignorance of the actual configuration by replacing the occupation numbers  $C_A(l)$  with the average concentration  $X_A$ . Of course  $[C_A(l)]^2 = X_A$  also. This is the Virtual Crystal Approximation (VCA), and we expect its application to well describe collective features such as long wavelength coupled oscillations when the wavelength is much greater than the average impurity spacing. Thus the random system is approximated by a periodic one and it is possible to treat the spatial Fourier transform propagator defined by

$$D^A(l\mu, l'\mu'; i\omega_n) = \frac{1}{N} \sum_{\vec{k}} e^{i\vec{k} \cdot (\vec{l} - \vec{l}')} D_{\mu\mu'}^A(\vec{k}, i\omega_n), \dots \dots \dots (27)$$

where  $N$  is the number of lattice sites per unit volume.

We also define

$$\Phi_{\mu\mu'}(l l') = \frac{1}{N} \sum_{\vec{k}} \Phi_{\mu\mu'}(\vec{k}) e^{i\vec{k} \cdot (\vec{l} - \vec{l}')} \dots \dots \dots (28)$$

Then since

$$\partial_{ll'} = \frac{1}{N} \sum_{\vec{k}} e^{i\vec{k} \cdot (\vec{l} - \vec{l}')}$$

Eq. (26) becomes

$$\begin{aligned}
 D_{\mu\mu'}^A(\vec{k}, i\omega_n) &= D_0(i\omega_n) \partial_{\mu\mu'} + \frac{1}{m_A\omega_A} \\
 & X_A \Phi_{\mu\mu'}(\vec{k}) [D_0^A(i\omega_n)]^2 \\
 & + \frac{1}{(2m_A\omega_A)^2} X_A^2 \sum_{\mu_1} \Phi_{\mu\mu_1}(\vec{k}) \Phi_{\mu_1\mu'}(\vec{k}) \\
 & [D_0^A(i\omega_n)]^3 + \dots \dots \dots (29)
 \end{aligned}$$

But we note that  $\Phi_{\mu\mu'}(\vec{k})$  is just related to the dynamical matrix  $D(\vec{k})$  by

$$\Phi_{\mu\mu'}(\vec{k}) = m_A D_{\mu\mu'}(\vec{k}), \dots \dots \dots (30)$$

and in the long wavelength limit, which will be our concern when the effects of the electron gas are considered, one finds through making use of the Ewald transformation (Born, 1954)

$$D_{\mu\mu'}(\vec{k}) = \Omega_A^2 \left( \frac{K_\mu K_{\mu'}}{K^2} - \frac{1}{3} \partial_{\mu\mu'} \right) + \theta(K^2). \dots \dots \dots (31)$$

Here  $\Omega_A = [4\pi N e^2 / \epsilon_\infty m_A]^{\frac{1}{2}}$  is the ion plasma frequency. We limit Eq. (29) to the case that  $\mu' = \mu$ . Then we have simply

$$\begin{aligned}
 D_{\mu\mu}^A(\vec{k}, i\omega_n) &= D_0^A(i\omega_n) \left[ 1 - \frac{1}{2m_A\omega_A} \right. \\
 & \left. X_A \Phi_{\mu\mu}(\vec{k}) D_0^A(i\omega_n) \right]^{-1} \dots \dots \dots (32)
 \end{aligned}$$

Thus by Eqs. (30) and (31) and analytically continuing  $i\omega_n$  to  $\omega$ , we find in the long wavelength limit,

$$\begin{aligned}
 D_{\mu\mu}^A(\vec{k} \rightarrow 0, \omega) &= 2\omega_A / [\omega^2 - \omega_A^2 \\
 & - X_A \Omega_A (K_\mu^2 / K^2 - \frac{1}{3})], \dots \dots \dots (33)
 \end{aligned}$$

so that the coupled mode frequencies, given by the poles of the Green's function, are shifted by the last term in the denominator. Now when  $\vec{K}$  is parallel to the ion displacements we have

$$D_{\mu\mu}^A(\omega) = 2\omega_A / [\omega^2 - \omega_A^2 - \frac{2}{3} X_A \Omega_A^2], \dots \dots \dots (34. a)$$

and when  $\vec{K}$  is perpendicular to the ion displacements the propagator becomes

$$D_{\mu\mu}^A(\omega) = 2\omega_A / [\omega^2 - \omega_A^2 + \frac{1}{3} X_A \Omega_A^2]. \dots \dots \dots (34. b)$$

Thus we have shown that the triply degenerate local modes are split by their mutual interactions into a nondegenerate upshifted longitudinal mode and a doubly degenerate downshifted transverse mode:

$$\omega^2 = \begin{cases} \omega_A^2 + \frac{2}{3} X_A \Omega_A^2, & \vec{K} \parallel \text{ion displacements} \\ \omega_A^2 - \frac{1}{3} X_A \Omega_A^2, & \vec{K} \perp \text{ion displacements.} \end{cases} \dots \dots \dots (33)$$

These results have been obtained previously (Maradudin, 1969) in a different context using the techniques of lattice dynamics. We emphasize that Eqs. (33)-(35) depend on the long wavelength approximation of Eq. (31), but Eq. (32) is exact

within the VCA.

The above results will be important in treating the more complex systems of (ii) and (iii), and we will find it convenient to proceed with the aid of Feynman diagrams which we now introduce. If the diagrams of Figure (1.a) are utilized, the expansion of Eqs. (26) or (29) can be expressed as shown in Figure (1.b), and the solution given in Eq.(32) is equivalent to the Dyson equation shown in Figure (1.c).

(ii) We now turn to a consideration of the two ion system defined by

$$H = H_A + H_{AA} + H_B + H_{BB} + H_{AB}, \dots (36)$$

One may proceed exactly as in (i) and again calculate the resonant modes of this system by obtaining the same Green's function defined in Eq.(21). For later notational clarity we now denote this propagator with a double superscript,  $D^{AA}$ . The propagator  $D^{BB}$  has an analogous form:

$$D^{BB}(I\mu\tau, I'\mu'\tau') = -\langle T_r [\varphi_{\mu}^B(I\tau) \varphi_{\mu'}^B(I'\tau')] \rangle, \dots (37)$$

where

$$\varphi_{\mu}^B(I) = b_{I\mu}^+ + b_{I\mu}$$

It is straightforward to expand  $D^{AA}$  in terms of  $D^A$  given by Figure(1.c), a similar propagator  $D^B$  and the interaction term  $H_{AB}$ . The results of such an expansion are summarized in Figure (2). As is clear from the structure of  $H_{AB}$  which is linear in  $\varphi_{\mu}^A(I)$  and  $\varphi_{\mu'}^B(I')$ , corrections to  $D^{AA}$  must contain only even powers of the interaction potential, and in fact all possible terms are accounted for by the Dyson equation of Figure (2.c). The solution of the Dyson equation yields the following analytic expression

$$D_{\mu\mu'}^{AA}(\vec{k}, \omega) = D_{\mu\mu'}^A(\vec{k}, \omega) \left\{ 1 - \frac{X_A X_B \Phi_{\mu\mu'}^2(\vec{k}) D_{\mu\mu}^A(\vec{k}, \omega) D_{\mu\mu}^B(\vec{k}, \omega)}{[2m_A \omega_A + 2m_B \omega_B]} \right\}^{-1} \dots (38)$$

An analogous propagator  $D^{BB}$  can be obtained directly from Eq. (38) by the interchange of subscripts A and B. Of course the denominators are symmetric under this interchange, reflecting the fact that the motions of the two ion species are coupled to each other.

Although we can obtain the resonant frequencies we seek from the propagator given in Eq.(38), For future reference we also list a new mixed ion propagator that has no zero order term. It is

$$D^{AB}(I\mu\tau, I'\mu'\tau') = -\langle T_r [\varphi_{\mu}^A(I\tau) \varphi_{\mu'}^B(I'\tau')] \rangle, \dots (39)$$

and expansion of this expression in an identical fashion as employed for  $D^{AA}$  yields the result shown in Figure (2.d). The corresponding analytic term is thus

$$D_{\mu\mu'}^{AB}(\vec{k}, \omega) = X_A X_B \Phi_{\mu\mu'}(\vec{k}) D_{\mu\mu}^A(\vec{k}, \omega) D_{\mu\mu}^B(\vec{k}, \omega) / [2m_A \omega_A + 2m_B \omega_B]^{\frac{1}{2}} X \left\{ 1 - X_A X_B \Phi_{\mu\mu'}^2(\vec{k}) D_{\mu\mu}^A(\vec{k}, \omega) D_{\mu\mu}^B(\vec{k}, \omega) / [2m_A \omega_A + 2m_B \omega_B] \right\}^{-1} \dots (40)$$

This mixed ion propagator will be seen to play a role in the alloy-electron gas system.

As in the single ion type case, one obtains characteristic longitudinal and transverse modes in this alloy system by finding the poles of any of the propagators  $D^{AA}, D^{BB}$  or  $D^{AB}$ . Again in the long wavelength limit, we may use Eq. (31) to obtain from Eq. (38) or (40) the following resonant frequencies

$$\omega_{\mu}^{\pm 2} = \frac{1}{2}(\omega_{\mu}^{A2} + \omega_{\mu}^{B2}) \pm \frac{1}{2} \left[ (\omega_{\mu}^{A2} - \omega_{\mu}^{B2})^2 + \frac{16}{9} X_A X_B \Omega_A^2 \Omega_B^2 \right]^{\frac{1}{2}} \dots (41. a)$$

and

$$\omega_{\pm}^{\pm 2} = \frac{1}{2}(\omega_{\pm}^A + \omega_{\pm}^B) \pm \frac{1}{2} \left[ (\omega_{\pm}^A - \omega_{\pm}^B)^2 + \frac{4}{9} X_A X_B \Omega_A^2 \Omega_B^2 \right]^{\frac{1}{2}} \dots (41. b)$$

Here we have defined  $\omega_{\mu}^{A2} \equiv \omega_A^2 + \frac{2}{3} X_A \Omega_A^2$ ,  $\omega_{\mu}^{B2}$

$$\equiv \omega_B^2 + \frac{2}{3} X_B \Omega_B^2, \omega_1^A \equiv \omega_A^2 - \frac{1}{3} X_A \Omega_A^2 \text{ and } \omega_1^B \equiv \omega_2^B - \frac{1}{3} X_B \Omega_B^2.$$

The B ion plasma frequency is  $\Omega_B = [4 \pi N e^{*2} / \epsilon_{\infty} m_B]^{\frac{1}{2}}$ . It should be noted that the sum rule for the single ion species system breaks down in the alloy system, and one finds from Eq. (41. a) and (41. b)

$$(\omega_{\vec{r}}^+ \omega_{\vec{r}}^-)^2 - (\omega_1^+ \omega_1^-)^2 = \omega_A^2 X_B \Omega_B^2 + \omega_B^2 X_A \Omega_A^2. \dots\dots\dots(42)$$

These results are displayed schematically in Figure (3), where the resonant frequencies of Eq. (41) are plotted as functions of the A ion concentration. The dashed diagonal lines show the modes that would result if each ion species interacted only with other ions of its own type, i.e.  $\omega_{\vec{r}}^A, \omega_{\vec{r}}^B, \omega_1^A$  and  $\omega_1^B$ . The two longitudinal modes are seen to mutually "repe" each other as do the two transverse modes.

When numbers appropriate to GaAs<sub>1-x</sub>P<sub>x</sub> (see Table 1) are inserted into Eq. (41), one finds the effect of  $H_{AB}$  to be small: The difference between  $\omega_{\vec{r}}^+$  and  $\omega_{\vec{r}}^A$  (here the A ions are phosphorus ions), with  $X_A = 0.5$  is found to be about  $1 \text{ cm}^{-1}$ . It may be that other alloy systems show a stronger coupling; we have yet to explore this possibility. It is obvious, however, that enhanced coupling will result if the localized frequencies of the respective isolated ion types are not greatly different. Further, anticipating the results of subsection(iii), we note that enhanced coupling can be expected if there is a means of "pushing the resonant frequencies closer together. There is such a method, and that is to introduce the electron gas, the subject to which we now turn.

(iii) In treating the fully interacting alloy-electron gas system it is possible to obtain the resonant frequencies by again calculating the Green's function defined in Eq. (21) as we have done in the two preceding sections. However it

is more convenient, and the resulting expression more symmetric, to instead introduce the electron density fluctuation propagator. It is given by

$$\chi(X\tau, X'\tau') = -\langle T_{\tau} [\delta_n(X\tau) \delta_n(X'\tau')] \rangle. \dots\dots\dots(43)$$

Here  $\delta_n(X\tau) = e^{H\tau} \delta_{n(X)} e^{-H\tau}$ , with H the full Hamiltonian given in Eqs. (2), (3) and (9), and  $\delta_{n(X)}$  is the density fluctuation propagator

$$\delta n(\vec{X}) = 4^+(X)4(X) - \langle 4^+(X)4(X) \rangle. \dots(44)$$

It is well known that the propagator  $\chi$  provides a description of the interacting electron gas (Fetter, 1971). In particular, if the electron density is sufficiently high, the use of the Random Phase Approximation (RPA) is justified, and the density fluctuation propagator has a particularly simple form. If the ion-electron interactions are temporarily ignored so that only  $H_{EE}$  contributes to the expansion of  $\chi$ , one has the series shown in Figure(4). Here  $\chi$  is represented by the "hatched" electron-hole bubble,  $\chi_0$  is a bare electron-hole bubble, and each power of  $H_{EE}$  contributes a dashed interaction line.

We note that if the Fourier transform of  $\chi$  is defined by

$$\chi(X\tau, X'\tau') = \frac{1}{\beta} \sum_{\vec{K}} \sum_{\omega_n} e^{i\vec{K} \cdot (\vec{X} - \vec{X}')} e^{-i\omega_n(\tau - \tau')} \chi(\vec{k}, i\omega_n), \dots(45)$$

the zero order term  $\chi_0(\vec{k}, i\omega_n)$  is expressed in terms of the free electron propagator  $G(\vec{k}, i\omega_n)$  as

$$\chi_0(Q, i\Omega_m) = \frac{3}{\beta} \sum_{\vec{K}} \sum_{\omega_n} G(\vec{k}, i\omega_n) G(\vec{k} + \vec{Q}, i\omega_n + i\Omega_m). \dots\dots(46)$$

The factor of two in Eq. (46) accounts for the electron spin.

The free electron propagator itself is defined by

$$G(\vec{X}\tau, \vec{X}'\tau') = -\langle T_{\tau} [4(\vec{X}\tau)4^+(\vec{X}'\tau')] \rangle, \dots\dots\dots(47)$$

and its Fourier transform of course has its poles at the allowed energies of the conduction band:

$$G(K, i\omega_n) = [i\omega_n - (K^2/2m^*) - \mu]^{-1}. \quad \dots\dots\dots(48)$$

Here  $\mu$  the chemical potential of the electron gas.

The essence of the RFA is to allow all contributions to  $\chi$  resulting from bubbles with internal structure to be neglected. (It is curious to note that the condition for the validity of the RPA is not satisfied for the polar semiconductors we consider here with typical electron concentrations  $\sim 10^{18} \text{ cm}^{-3}$  or less. The condition is simply  $r_s \geq 1$ , where  $r_s$  is a dimensionless measure of the electron density of the system:  $r_s = r_0/a_0$ , where  $n_e = (4\pi r_0^3/3)^{-1}$  and  $a_0$  is the Bohr radius. For semiconductors doped so that  $\omega_p$  is on the order of the optical vibration frequencies of the lattice,  $r_s$  is typically 0.2 or so, our approach is to use the RPA simply because the electron plasma is known to exist in the systems we treat in this paper, and, indeed, its properties are quantitatively well described by the RPA. The analytic expression corresponding to Figure (4) is simply

$$\chi(\vec{k}, \omega) = \chi_0(\vec{k}, \omega) / [1 - V_c(K)\chi_0(\vec{k}, \omega)]. \quad \dots\dots\dots(49)$$

The zero order term  $\chi_0$  is calculated exactly in the zero temperature limit while for finite temperatures only its imaginary part is expressible in an exact analytic form (Sirko, 1978).

It is possible, however, to represent the real part of  $\chi_0$  as an approximation to the zero temperature limit with only very minor quantitative error as long as the temperature is less than the Fermi temperature of the electron gas. The real part of  $\chi_0$  at absolute zero is given by the Lindhard function (Lindhard, 1954), and a realistic description of dispersion as well as the breakup of the electron plasma requires the use of Lindhard's formula in Eq. (49). However in this paper we will present only the longwavelength limit for which simple analytic expressions are obtainable. In section III we discuss the effects one expects

from a consideration of finite wave vector excitations, a topic we are now investigating quantitatively through numerical analysis.

When  $K \rightarrow 0$ ,  $\chi_0(K, \omega)$  has a very simple form (Fetter, 1971):

$$\chi_0(K \rightarrow 0, \omega) = \frac{n}{m^*} \frac{K^2}{\omega^2}, \quad \dots\dots\dots(50)$$

so that the long wavelength limit of  $\chi$  from Eq. (49) is seen to be

$$\chi(K \rightarrow 0, \omega) = (n/m^*)K^2 / [\omega^2 - \omega_p^2]. \quad \dots\dots(51)$$

Thus it is clear that in the long wavelength limit  $\chi$  itself can be thought of as a plasma propagator with its singularity at the collective resonant frequency of the electron gas.

To this point we have considered the ions and their mutual interactions, and we have introduced the electron density fluctuation propagator as a means of characterizing the interacting electron gas. We now show that it is a straightforward matter to combine the electrons and ions. For this purpose it is helpful to note that the electron-ion interaction terms,  $H_{AE}$  and  $H_{BE}$ , give rise to effective electron-electron interactions. This is obvious when one compares Figures (5.a) and (5.b). In Figure (5.a) the electron-electron interaction via  $H_{EE}$  is shown, while an analogous scattering involving  $H_{AE}$  can be seen to occur as in Figure (5.b). It is clear that within an RPA the exact density fluctuation propagator must contain terms as shown in Figure (5.c), which displays all RPA corrections to  $\chi_0$  that involve a single electron-electron scattering as well as a representative higher order term. Now,  $\chi$ , defined in Eq. (43) and including ion effects is drawn as a crosshatched bubble.

It is important to note that since the electron plasma oscillations are longitudinal, it is the longitudinal ion vibrations which couple to the electron gas. This result of course is guaranteed by the dependence of  $H_{AA}$  on the component of  $\vec{q}$  in the direction of ion displacement in Eq. (16).



Again within the RPA one finds that a Wick's theorem expansion of  $\chi$  can be expressed concisely as in figure(5.d). this is a key result, and the corresponding analytic expression is

$$\chi(\vec{k}, \omega) = \chi_p(\vec{k}, \omega) \left\{ 1 - \frac{\chi_p(\vec{k}, \omega)}{K^2} \left[ NX_A \gamma_A^2 D_p^{AA}(\vec{k}, \omega) + NX_B \gamma_B^2 D_p^{BB}(\vec{k}, \omega) + 2N\gamma_A \gamma_B D_p^{AB}(\vec{k}, \omega) \right] \right\}^{-1} \quad (52)$$

Here we have denoted the electron density fluctuation propagator that results when only  $H_{EE}$  contributes to electron scattering as  $\chi_p$ . It is given by Eq.(49). The actual procedure used in obtaining Eq. (52) was to calculate directly the first order corrections to  $\chi$  by a Wick's theorem expansion and thus obtain the correct coupling constants above. The diagrammatic analysis of Figurs(5) then permits direct generalization to the infinite order expansion given above. We emphasize that in its present form Eq.(52) is correct for all  $\vec{k}$ . Thus, realistic computation of dispersion depends only on representing  $\chi_0(\vec{k}, \omega)$  accurately. As noted previously the dispersion due to  $\Phi(K)$  is negligible for the entire region in which the electron gas exhibits plasma like behavior.

Again specializing to the long wavelength limit we take the  $K \rightarrow 0$  values of  $\chi_0$  and  $\Phi$  given by Eqs. (31) and (50), substitute into Eqs. (38), (40) and (49) and use these expressions in Eq.(52). Then after some rearrangement one finds that the poles of  $\chi$  occur at the frequencies which satisfy

$$\omega^6 - \omega^4(\omega_A^2 + \omega_B^2 + \omega_p^2) + \omega^2 \left[ \omega_p^2(\omega_A^2 + \omega_B^2) + \omega_A^2 \omega_B^2 - \frac{4}{9} X_A X_B \Omega_A^2 \Omega_B^2 \right] - \omega_p^2 \left( \omega_A^2 \omega_B^2 - \frac{X_A X_B}{9} \Omega_A^2 \Omega_B^2 \right) = 0 \quad (53)$$

Using parameters appropriate to  $n$ - $G_A A_{S1} \cdot X P_X$

as displayed in Table 1, we graph in Figure (6) the variation of the resonant mode frequencies as a function of  $P$  ion concentration for a particular electron concentration. The dashed lines represent the modes that would result if the  $P$  and  $A_S$  ions interacted only with members of their own species. As was anticipated in (ii) one sees clearly that the modes are strongly mixed over nearly the entire range  $0 < X < 1$ .

Our work has assumed that the two ion species  $A$  and  $B$  are isoelectronic, while for a real crystal this assumption must be slightly relaxed. In obtaining the numerical results we have treated  $\epsilon_\infty$  as a varying parameter with limiting values appropriate to Ga As at  $X=1$  and to  $G_s P$  at  $X=1$ . Then the values of  $\omega_p^{A2}$  and  $\omega_p^{B2}$  in Eq.(53) are found from

$$\omega_p^2 = \frac{1}{3} (\omega_L^2 + 2\omega_T^2) + X(\omega_L^2 - \omega_T^2), \dots$$

where  $\omega_L$  and  $\omega_T$  are given in Table 1 and  $X$  is either  $X_A$  or  $X_B$ .

In Figure (7) is shown the frequency variation of the three resonant modes as a function of electron concentration for a particular alloy composition. The slight repulsion due to the mutual A-B ion interactions when  $n_s=0$  as derived in (ii).

Again, there is a fairly broad region in  $n_s$  over which vigorous mixing of all three modes is present. Additionally, one notes that in the high electron density limit the "ion like" modes approach not the longitudinal optical frequencies but the transverse optical frequencies. This is simply a consequence of the screening of the individual ion sites of the high density electron gas thus effectively blocking the ion-ion interactions that would otherwise upshift the frequencies to the longitudinal values.

In addition to the three strongly interacting longitudinal modes described here, the transverse ion modes, calculated in (ii), are unaffected by

the electron gas.

### III. DIELECTRIC CONSTANT

For some applications such as calculating absorptivity it may be useful to have an expression for the dielectric constant of the alloy-electron gas system. The dielectric constant may be most easily obtained from the expression

$$V_{eff}(\vec{K}, \omega) = V_0^b(K) / \epsilon(\vec{K}, \omega), \dots\dots\dots(54)$$

where  $V_0^b(K)$  is the bare Coulomb potential,  $V_0^b(K) = 4\pi e^2 / K^2$ ,  $\epsilon(\vec{K}, \omega)$  is the dielectric constant and  $V_{eff}(\vec{K}, \omega)$  is the effective electron-electron interaction potential. Figure (8) outlines the diagrammatic development of the effective potential.

In Figure (8.a) the effective potential is expanded in terms of the simple scattering processes we have already described. Then with the definition of  $V_{eff}^0(\vec{K}, \omega)$  in Figure (8.b), we obtain the RPA approximation of the effective potential as shown in Figure (8.c). By definition

$$\begin{aligned} V_{eff}(\vec{K}, \omega) = & \frac{4\pi e^2}{\epsilon_\infty K^2} + NX_A \gamma_A^2 D^{AA}(\vec{K}, \omega) / K^2 \\ & + NX_B \gamma_B^2 D^{BB}(\vec{K}, \omega) / K^2 \\ & + 2N\gamma_A \gamma_B D^{AB}(\vec{K}, \omega) / K^2, \\ & \dots\dots\dots(55) \end{aligned}$$

where we use the same coefficients found in the expansion of  $\chi$  in section II. Thus by the Dyson equation of Figure (8.c) we have

$$\begin{aligned} V_{eff}(\vec{K}, \omega) = & V_{eff}^0(\vec{K}, \omega) / [1 - V_{eff}^0(\vec{K}, \omega) \\ & \chi_0(\vec{K}, \omega)], \dots\dots\dots(56) \end{aligned}$$

and by Eq. (54),

$$\begin{aligned} [\epsilon(\vec{K}, \omega)]^{-1} = & \frac{V_{eff}^0(\vec{K}, \omega)}{V_0^b(K)} \left\{ 1 - V_{eff}^0(\vec{K}, \omega) \right. \\ & \left. \chi_0(\vec{K}, \omega) \right\}^{-1} \dots\dots\dots(57) \end{aligned}$$

### IV. CONCLUDING REMARKS

We have developed the formalism describing

the nature of coupling in a polar semiconductor binary alloy-electron gas system, and have carried out numerical calculations for a representative real crystal in the long wavelength limit. We have seen that the mixing of the elementary excitations is significant over a broad range of ion and electron concentrations.

Although the effects of dispersion have not been numerically calculated, the general formalism contains the wave vector dependency, and interesting effects can be expected by probing finite wavelength excitations. Qualitatively it is clear that as the wave vector is increased from zero the coupled mode frequencies will shift due to the strong dependence of the electron plasma on the wave vector. Then as the wave vector increases significantly beyond the Debye inverse screening length the three strongly coupled modes we have described should rapidly change: the plasma like mode must decay into the single particle excitations of the Landau damping region, and the other two modes must shift back to the nearly uncoupled modes described in section II (ii). Detailed analysis of these shifts requires numerical computations which we expect to carry out. Raman scattering should provide an excellent means of probing the effects we have have quantitatively described in section II and qualitatively described in this section. In addition, selection of particular geometries should allow both the longitudinal strongly coupled modes and the transverse weakly coupled modes to be studied in turn with the same specimen. A future paper will treat the wave vector dependent effects and apply the formalism developed here to the Raman scattering problem.

### ACKNOWLEDGEMENTS

This work was supported in part by a grant from the Ministry of Education.

(TABLE 1)

	$\omega_L$	$\omega_T$	$\omega_0^*$	$\Omega_0^+$
GaP	403*	367*	379	166
GaAs	292*	269*	277	144(cm <sup>-1</sup> )
	* $\omega_0(\text{GaP}) \equiv \omega_A$ ; $\omega_0(\text{GaAs}) \equiv \omega_B$			
	+ $\Omega_0(\text{GaP}) \equiv \Omega_A$ ; $\Omega_0(\text{GaAs}) \equiv \Omega_B$			
	≠ see reference (14)			

### FIGURE CAPTIONS

Figure 1. (a) The Feynman diagrams of (i) are built from the elements defined here. (b) The expansion of the exact Green's function in terms of the zero order Green's function and the interionic potential. (c) Dyson's equation from which an expression for the exact propagator is obtained.

Figure 2. (a) Propagators used in a B ion system. (b) The B ion displacement propagator Dyson equation. (c) The expansion of  $D^{AA}$  in an A-B ion alloy including all possible interionic interactions. (d) The Dyson equation for the mixed ion propagator  $D^{AB}$ .

Figure 3. The resonant modes  $\omega_L^\pm$  and  $\omega_T^\pm$  as a function of A ion concentration. The dashed lines represent the values appropriate when  $H_{AB} \rightarrow 0$  so that each ion type interacts only with members of its own species. The values  $\omega_{LA}(\omega_{LB})$  and  $\omega_{TA}(\omega_{TB})$  are the longitudinal and transverse optical frequencies of the pure A (B) ion lattice. For the interacting alloy system the longitudinal modes are seen to mutually repel each other as do the transverse modes.

Figure 4. The RPA expansion of the electron density fluctuation propagator. All terms containing electron-hole bubbles with internal struc-

ture are neglected. Ion effects are not included here. The shaded bubble is the exact Green's function,  $\chi$ , when only electron-electron effects are present. The bare bubbles are the zero order approximation,  $x_0$ , and the dashed lines are the Coulomb potential terms.

Figure 5. (a) Electron-electron scattering process arising from the Coulomb interaction  $H_{EE}$ . (b) An equivalent electron-electron scattering process involving a second order local mode process (creation and destruction of a local mode excitation). (c) The first few terms in the expansion of  $\chi$  involving both electron and ion effects. (d) The Dyson equation for  $\chi$  in terms of the plasma propagator defined in Eq. (49) (the shaded electron-hole bubble on the right hand side), and the interionic propagators derived in (ii).

Figure 6. The coupled longitudinal modes in n-GaAs<sub>1-x</sub>P<sub>x</sub> as a function of  $x$ . The dashed lines indicate the modes that would result without ion-electron and A-B ion coupling. Here parameters given in Table 1 were used along with an electron concentration such that  $\omega_p = 385 \text{ cm}^{-1}$ . (This corresponds to  $n_e = 1.15 \times 10^{18} \text{ cm}^{-3}$  in GaAs.)

Figure 7. The coupled longitudinal modes in n-GaAs<sub>0.5</sub>P<sub>0.5</sub> as a function of  $n_e$ . Here the frequencies are calculated in terms of  $\omega_L$  given in Table 1 for GaP.

Figure 8. (a) The first few terms of an expansion of the effective electron-electron scattering potential. (b) The definition of an "effective zero order scattering potential." (c) An expansion of the effective potential in terms of the potential defined in (b).

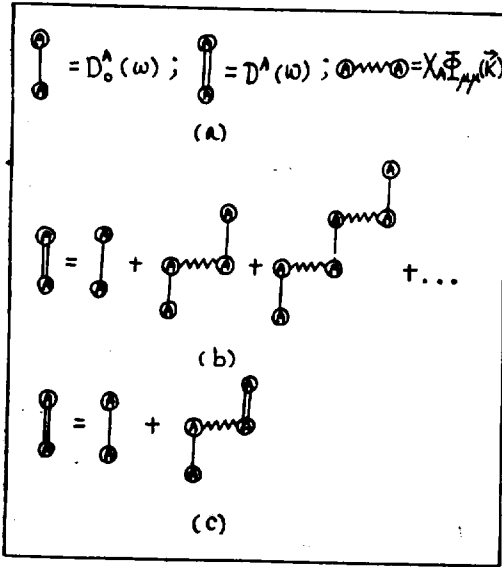


Fig. 1.

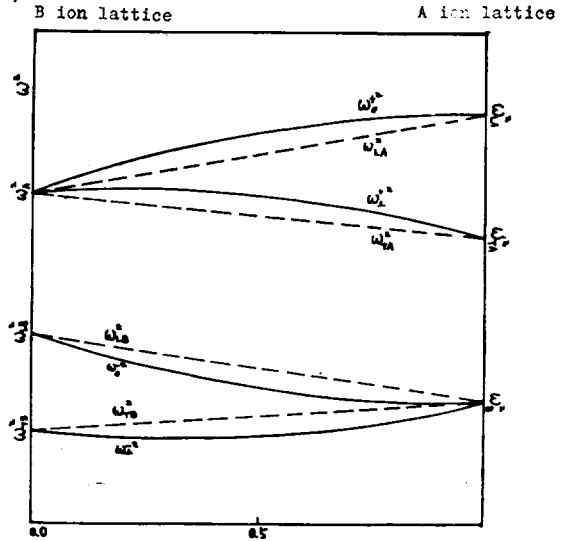


Fig. 3.

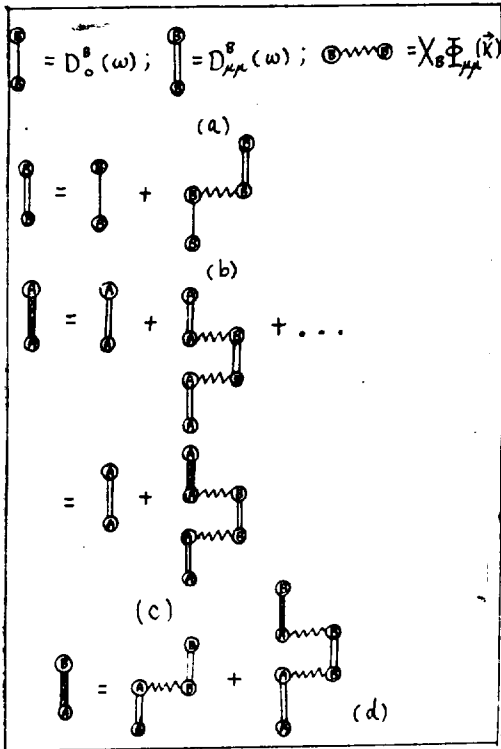


Fig. 2.

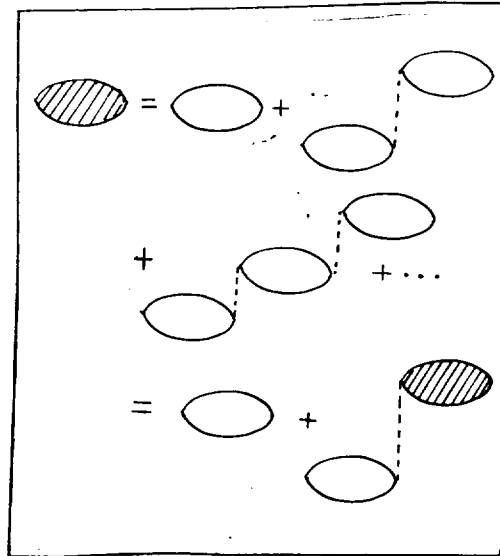


Fig. 4.

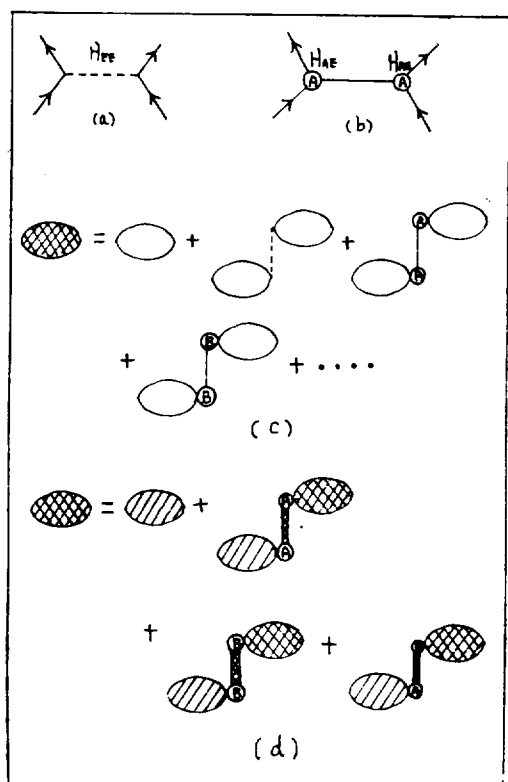


FIG. 5.

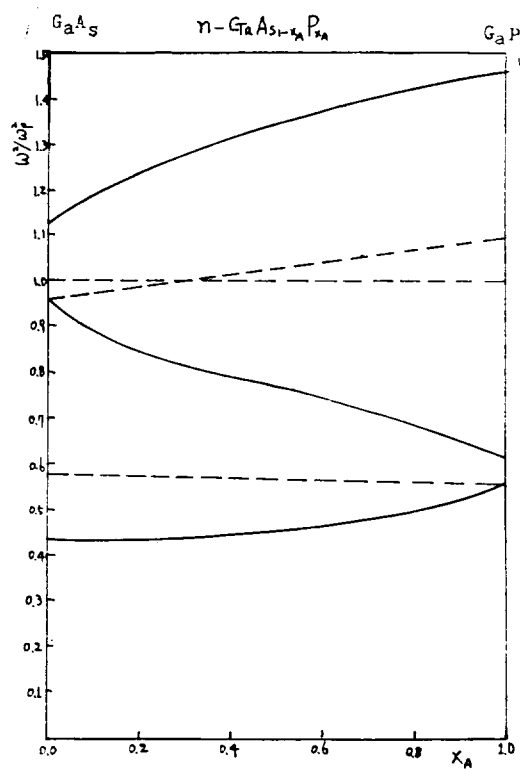


FIG. 6.

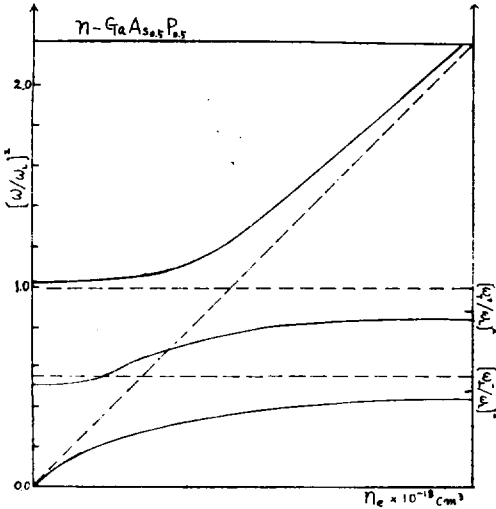
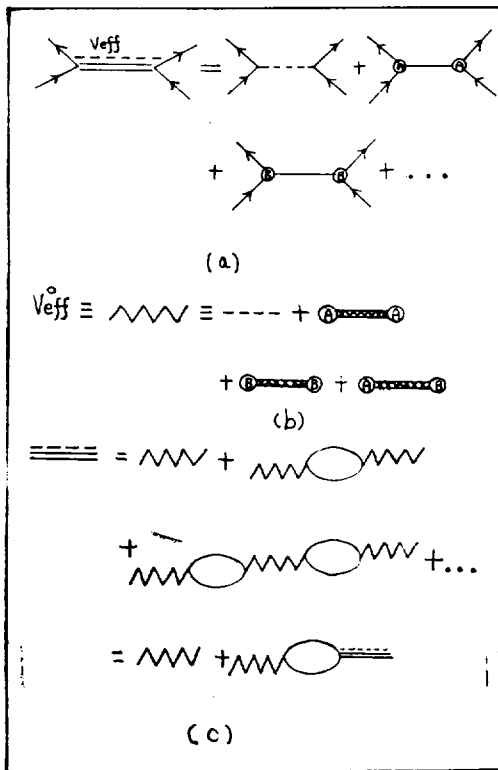


Fig. 7.



REFERENCES

A. A. Maradudin and J. Oitmaa, *Solid State Commun.* **7**, 1143, (1969).  
 A. F. Fetter and J. D. Walecka, *Quantum Theory of Many Particle Systems*, McGraw Hill, New York (1971).  
 A. Mooradian and A. L. McWhorter, *Proc. of Int. Conf. on Light Scattering Spectra of Solids*. (Edited by G. B. Wright, 1968) Springer-Verlag, 1969.  
 A. Mooradian and G. B. Wright, *Phys. Rev. Lett.* **16**, 999 (1966).  
 E. W. Montroll and R. B. Potts, *Phys. Rev.* **100**, 525 (1955).  
 J. Lindhard, *Kgl. Danske Videnskab. Selskab. Mat. Fis. Medd.* **28**, 408 (1954).  
 K. S. Singwi and M. P. Tosi, *Phys. Rev.* **147**, 658 (1966).  
 L. J. Sham and A. A. Maradudin, *Solid State Commun.* **5**, 337, (1967).  
 M. Born and K. Huang, *Dynamical Theory of Crystal Lattices*, O. U. P., New York (1954).  
 R. Sirko and D. L. Mills, *Phys. Rev. B* **18**, 4373 (1978).  
 R. Sirko, K. R. Subbaswamy and D. L. Mills, *Phys. Rev. B* **18**, 851 (1978).  
 S. Katayama, Ph. D. Thesis (Osaka University, Toyonaka, 1975) (unpublished).  
 See, for example, A. A. Abrikosov, L. P. Gorkov and I. Ye. Dzyaloshinski, *Quantum Field Theoretical Methods in Statistical Mechanics* (Pergamon, New York, 1965).  
 W. Hayes and R. London, *Scattering of Light by Crystals*, Wiley, New York (1978).